

# A stabilized pairing functional

J. Erler<sup>1</sup> and P. Klüpfel<sup>1</sup> and P.-G. Reinhard<sup>1</sup>

Institut für Theoretische Physik, Universität Erlangen, Staudtstrasse 7, D-91058 Erlangen, Germany

October 26, 2018/ Received: date / Revised version: date

**Abstract.** We propose a modified pairing functional for nuclear structure calculations which avoids the abrupt phase transition between pairing and non-pairing states. The intended application is the description of nuclear collective motion where the smoothing of the transition is compulsory to remove singularities. The stabilized pairing functional allows a thoroughly variational formulation, unlike the Lipkin-Nogami (LN) scheme which is often used for the purpose of smoothing. First applications to nuclear ground states and collective excitations prove the reliability and efficiency of the proposed stabilized pairing.

**PACS.** 2 1.10.Dr, 21.10.Re, 21.30.-x, 21.60.-n, 74.20.Fg

## 1 Introduction

Pairing is a key ingredient in a mean field description of nuclear structure [1]. The actual handling has much evolved. Early models referred to simple forms assuming a constant gap or constant pairing matrix element [2]. Modern nuclear mean field calculations use a fully fledged pairing force, often even density dependent, for an up to date review see [3]. In any case, the theoretical description relies on an extended notion of a mean field, now including the two-quasi-particle density and gap-potential also at mean field level. That allows to include a crucial part of two-particle correlations at low expense. The price to be paid for that simplification is the occurrence of a pairing phase transition. Whenever the pairing strength crosses a critical value, the system jumps from a pairing to a non-pairing state or vice versa. For finite system such a sudden transition is an artefact [4]. A fully correlated treatment would produce correctly smoothed transitions. That goal of smoothing can already be achieved when working with a particle-number projected pairing state, provided the mean-field variation is done after projection (VAP). For then the system takes advantage of the pairing channel to incorporate some correlations “knowing” that the exact particle number will be restored. But the VAP method is cumbersome and not applicable in connection with energy functionals [5]. Thus one employs usually simpler approaches which then are plagued by phase transitions. These are bearable when tracking ground states of nuclei where the change in nucleon number is discontinuous anyway. However, they turn into a severe problem when going along continuous changes as one does for large amplitude collective motion, see e.g. [3, 6, 7]. A sudden phase transition along the collective evolution leads to unwanted singularities in the description. Within the adiabatic treatment of large-amplitude collective motion, one encoun-

ters, e.g., singularities in the collective masses. A phase transition would be even more disastrous for fully time-dependent mean-field calculations which enjoy a revival those days, see e.g. [8, 9]. Thus there is a need to smoothen the sudden pairing phase transition. A widely used recipe is the Lipkin-Nogami (LN) scheme [10, 11] which aims at an approximate treatment of particle-number projection and this approximation has the similar smoothing effects as the exact projection in VAP. Thus most of the microscopic calculations of large-amplitude collective motion employ LN pairing to generate the underlying series of collectively deformed states, see e.g. [12, 13, 14, 15]. However, the LN prescription has still a few disadvantages in these large-scale applications: it introduces complicated terms and one more equation into the pairing scheme; the necessary feed-back on the self-consistent mean field [16] slows down the computational speed and degrades the numerical stability; it is not strictly variational which makes the validity of the LN approach less controllable. Moreover, the feature of approximate particle-number projection is not really exploited. If a precise particle number is a matter of concern, it is restored explicitly after the mean-field calculations. The superposition of mean-field states to a collective, or correlated, state requires anyway an explicit handling of particle number which is performed either by projection (e.g. [15]) or by adjustment in the average (e.g. [14]). As mentioned above, the formally perfect alternative of particle-number projection with subsequent mean-field variation (VAP) is inhibited in connection with the Skyrme-Hartree-Fock functional [5]. There is thus a need for a conceptually simple, variationally consistent, and numerically stable recipe to avoid, or smoothen, the pairing phase transition, particularly for the simulation of large-amplitude collective motion. It is the aim of this paper to present and to discuss a stabilized pairing functional which avoids the phase transition while inducing a mini-

mum of changes to other nuclear properties. The idea is to modify directly the pairing-energy functional such that a vanishing pairing gap becomes associated with infinitely increasing energy while merging into the ordinary pairing-energy functional in regions of well developed pairing gap such that standard pairing properties are not affected. The stabilized scheme is illustrated on a schematic two-level model. First realistic application to nuclear structure and collective excitations computed with the self-consistent Skyrme-Hartree-Fock (SHF) method will also be presented.

## 2 The stabilized functional

The standard procedure starts from an energy functional,  $E = E_{\text{mf}} + E_{\text{pair}}$ , consisting out of a mean-field part and an pairing functional. The energy depends on a set of single-particle wavefunctions  $\varphi_k$  and occupation amplitudes  $v_k$  with complementing non-occupation amplitudes  $u_k = \sqrt{1 - v_k^2}$ . Variation with respect to  $\varphi_k^*$  yields the mean-field equations and variation with respect to  $v_k$  the gap equation determining the pairing properties [2, 17]. The gap equation does not always have finite solution. There can emerge a phase transition to zero pairing gap and zero pairing energy. This induces singularities in the derivatives which spoils many applications as, e.g., the description of large-amplitude collective motion. The Lipkin-Nogami scheme (LN) avoids that sudden change by an additional term  $\propto \langle \hat{N}^2 \rangle$  in the energy, whereby  $\hat{N}$  is the operator for particle number (for a discussion in connection with self-consistent mean-field models see [16]). However, it has some disadvantages as discussed in the introduction. We propose to stabilize a finite pairing by introducing a counteracting term in the pairing energy functional. The stabilized pairing functional reads

$$E_{\text{pair}}^{(\text{stab})} = E_{\text{pair}} \left( 1 - \frac{E_{\text{cutp}}^2}{E_{\text{pair}}^2} \right) = E_{\text{pair}} - \frac{E_{\text{cutp}}^2}{E_{\text{pair}}} \quad (1)$$

It can be applied to any given pairing functional  $E_{\text{pair}}$ . It guarantees always a finite pairing because the term  $\propto E_{\text{pair}}^{-1}$  grows huge when pairing is on the way to breakdown. The stabilized function (1) introduces a new parameter, the cutoff pairing energy  $E_{\text{cutp}}$  which has to be chosen to deliver sufficient stabilization with minimal effects in the well pairing regime. The stabilized equations are derived as before by variation of the total energy, now

$$\delta E = \delta \left[ E_{\text{mf}} + E_{\text{pair}}^{(\text{stab})} \right] = 0 \quad (2a)$$

This yields the stabilized coupled mean-field and gap equations

$$\hat{h}\psi_k = \epsilon_k \psi_k \quad (2b)$$

$$2(\epsilon_k - \lambda)u_k v_k = \Delta_k^{(\text{stab})}(u_k^2 - v_k^2) \quad (2c)$$

$$\Delta_k^{(\text{stab})} = \Delta_k \left( 1 + \frac{E_{\text{cutp}}^2}{E_{\text{pair}}^2} \right) \quad (2d)$$

where  $\Delta_k$  is composed from the  $u_k, v_k$  as in regular BCS approach for the given functional. The detailed form depends on the actual system. It will be specified later on in connection with the examples.

## 3 Test in a two-level model

For a first exploration we employ a simple-most model for mean field plus pairing. We consider  $N$  particles in two energy levels, both  $N$ -fold degenerated. The levels are labeled by  $(s, m)$  where  $s \in \{u, l\}$  stands for the principle quantum number and  $m = \pm 1, \dots, \pm N/2$  accounts for the (degenerated) magnetic quantum numbers. The energy difference between upper and lower states,  $E_{\text{ul}} = \epsilon_u - \epsilon_l$  simulates the shell spacing. Pairing is added with a constant pairing force [2]. The occupation amplitudes are also degenerated  $v_{sm} = v_s$ . For symmetry reasons, we have  $v_l = v$ ,  $v_u = \sqrt{1 - v^2}$ , and  $u = \sqrt{1 - v^2}$ . This makes altogether the total energy

$$E = E_{\text{mf}} + E_{\text{pair}} \quad (3a)$$

$$E_{\text{mf}} = \frac{E_{\text{ul}}}{2} N(u^2 - v^2) \quad (3b)$$

$$E_{\text{pair}} = -G(Nuv)^2 \quad (3c)$$

The mean-field variation is obsolete because the single particle energies  $\epsilon_{u,l}$  are given. It remains the variation of pairing properties which yields the gap equation  $E_{\text{ul}}uv + \Delta(u^2 - v^2) = 0$  where  $\Delta = G N u v$ . Its solution for the gap becomes

$$\Delta = \frac{E_{\text{ul}}}{2} \sqrt{\left( \frac{NG}{E_{\text{ul}}} \right)^2 - 1} \quad (4)$$

The decisive parameter for the model is the ratio  $NG/E_{\text{ul}}$ . Pairing breaks down for  $NG/E_{\text{ul}} \leq 1$ . The breakdown should now be hindered by introducing the stabilized functional (1) which yields the stabilized gap as

$$\Delta^{(\text{stab})} = \frac{E_{\text{ul}}}{2} \sqrt{\left( \frac{NG}{E_{\text{ul}}} \right)^2 \left( 1 + \frac{E_{\text{cutp}}^2}{E_{\text{pair}}^2} \right)^2 - 1} \quad (5)$$

This is a rather involved equation for the gap because  $E_{\text{pair}}$  on the right hand side depends implicitly on  $\Delta$ . But the crucial result is that the expression under the square root can never vanish and thus the gap equation has always a finite real solution.

Figure 1 shows results of the two-level model for phase space  $N = 20$ . The pairing gaps are given in the upper panel. BCS produces a phase transition at relative coupling strength  $G/E_{\text{ul}} \approx 0.05$  and LN clearly removes that discontinuity producing a gap which smoothly approaches zero in the limit  $G \rightarrow 0$ . In the regime of active pairing, the LN gap approaches the BCS gap as it should. Both results from the stabilized functional (1) smoothen the transition, at first glance similar to LN. However, the functional behavior differs in detail. The trend at small  $G$  produces more efficient stabilization of the pairing gap, as can be seen, e.g., from the result for the extremely small

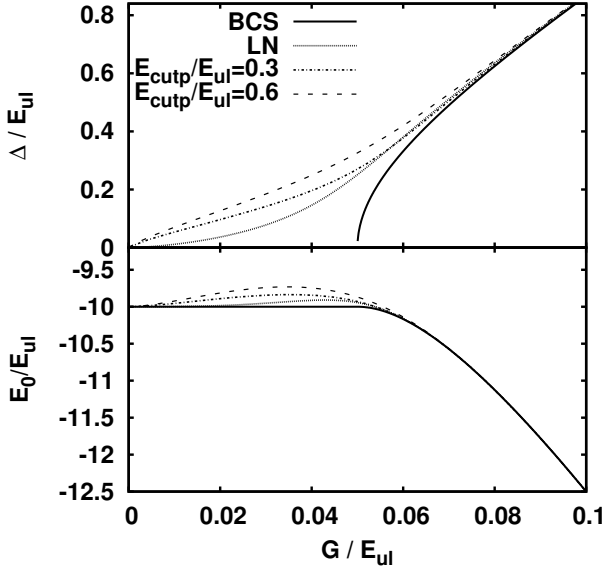


**Fig. 1.** Upper: Dependence of the pairing gap on the coupling strength for various methods in comparison, BCS, LN and the stabilized pairing with two different cutoff parameters as indicated. Lower: The total energy of the system as function of the coupling strength.

$G/E_{ul} = 0.01$ . At the side of active pairing, the stabilized functional also converges to the BCS curve where the speed of convergence improves with decreasing  $E_{cutp}$ . The goal is to have a slow decrease of  $\Delta$  for  $G \rightarrow 0$  combined with a fast convergence to BCS for large  $G$ . The stabilized pairing promises to provide here a better compromise than LN. The lower panel of figure 1 shows the binding energies. LN follows the BCS curve with a maximum deviation of 2% near the critical value  $G/E_{ul} \approx 0.05$ . The stabilized pairing shows also deviation which, however, extend further below the critical value. The maximum deviation depends sensitively on the cutoff energy. The smaller cutoff produces an error similar to LN and the larger cutoff has a larger error. Thus a good compromise will dwell at the lower side of cutoff energies. The actual choice will depend, of course, on the actual system and the intended applications.

The two-level model is based on an explicit Hamiltonian. This allows to perform particle-number projection. The most advanced approach is mean-field variation after projection (VAP). We compare that with the results from mean-field calculations where projection is done after mean-field variation. Figure 2 shows the results drawn as relative deviation from VAP because the differences for the projected results are too small to be seen when showing the total energies as such. The BCS case deviates most strongly below the critical coupling strength  $G$ . Pairing was not active here and no energy can be gained from pairing with subsequent projection. The deviation stays at the level of 3–4 % for pure mean-field results. The unprojected BCS curve shows the typical size and

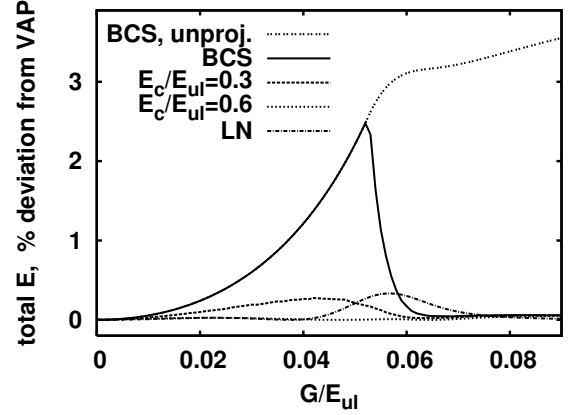


**Fig. 2.** Comparison of various approaches with variation after particle-number projection (VAP) for the total energy as observable drawn as % deviation from the VAP result versus the normalized coupling strength. Test case is again a system with particle number  $N = 20$ . The four cases, BCS, LN and stabilized BCS at two different cutoff energies employ particle-number projected calculations applied to the given mean field state (projection after variation = PAV). An unprojected mean-field result is also given for the case of BCS.

trend which looks very similar also for the (unprojected) other methods. The projected BCS result converges above the critical strength rapidly to a very small deviation. LN and stabilized gap show very small deviations throughout. The figure confirms that LN with subsequent projection is an efficient approach to full VAP. And it shows that the newly developed stabilized gap performs equally well, and sometimes better, in that perspective. The case of  $E_{cutp}/E_{ul} = 0.6$  shows that proper tuning may even enhance the quality. On the other hand, being satisfied with LN quality means that one disposes of a broad band of choices for  $E_{cutp}/E_{ul}$  which one can use to optimize other aspects as, e.g., stability.

## 4 Nuclear ground states and collective dynamics

### 4.1 The modified functional and BCS equations

Self-consistent nuclear mean-field models are based on effective energy-density functionals. The three most widely used models are the relativistic mean-field model (for reviews see e.g. [18,19,20]), the Gogny force (see e.g. [21]), and the Skyrme-Hartree-Fock (SHF) approach (for a recent review see e.g. [3]). We concentrate here on SHF. Although there had been attempts to incorporate pairing directly into the Skyrme force [22], most functionals keep mean-field and pairing properties separate. Recent SHF calculations employ generally a pairing functional derived

from a zero-range pairing force [23,24]. It reads

$$E_{\text{pair}} = \frac{1}{4} \sum_{\mathbf{q}} \int d^3r V_{\mathbf{q}}(\mathbf{r}) \chi_{\mathbf{q}}^2(\mathbf{r}) \quad , \quad (6a)$$

$$\chi_{\mathbf{q}}(\mathbf{r}) = 2 \sum_{k>0} f_k u_k v_k |\varphi_k(\mathbf{r})|^2 \quad , \quad (6b)$$

where  $f_k$  is a smooth cutoff function which limits the pairing space to an energy region up to 5 MeV above the Fermi energy [3,25]. That pairing functional is added to the SHF mean-field energy functional which is rather lengthy. We refer to [3,26] for details. The state-dependent pairing gap from this functional becomes

$$\Delta_k = -\frac{V_q}{2} \int d^3r \chi_{\mathbf{q}(\mathbf{k})}(\mathbf{r}) |\varphi_k(\mathbf{r})|^2 \quad . \quad (6c)$$

The gap equations derived from that functional show also the possible breakdown of pairing. We modify the functional (6a) to the stabilized pairing (1). As a consequence, we deal now with the stabilized equations (2). These will be solved in spherical symmetry for the ground states of spherical nuclei [27] and in axial symmetry for computing the collective deformation path and subsequent collective dynamics [14]. There is a broad variety of parameterizations of the SHF mean-field functional [3]. The actual choice is not crucial for the present tests of the stabilized pairing functional. We use here the parameterization SkI3 [28].

The pairing gap from the functional (6a) becomes state dependent as  $\Delta_k$ . In order to have one number characterizing the gap, we define an average pairing gap as

$$\bar{\Delta}_q = \frac{\sum_{k \in q} f_k u_k v_k \Delta_k}{\sum_{k \in q} f_k u_k v_k} \quad . \quad (7)$$

The weight factor  $u_k v_k$  concentrates averaging to a region near the Fermi energy where pairing is most relevant. That definition is found to be the most appropriate for comparisons [25].

## 4.2 Results and discussion

The uppermost two panels of figure 3 show proton and neutron pairing gaps along the semi-magic chain of Sn isotopes. The proton number  $Z=50$  is magic throughout the isotopic chain. Thus BCS proton pairing breaks down for all isotopes while LN and stabilized pairing produce a small but finite gap. The actual size of the stabilized gap depends somewhat on the chosen cutoff whereby the lower  $E_{\text{cutp}}$  produces results very close to LN. BCS neutron pairing drops to zero for the two magic neutron numbers  $N = 50$  and  $N = 82$ , has substantial pairing mid shell, and a short transitional region near the magic numbers. LN produces, of course, a finite gap at the magic points and tries to come close to BCS when going away from the shell closures. The results from stabilized pairing do also produce finite gaps at the shell closures. The actual value of the gaps there depend again somewhat on

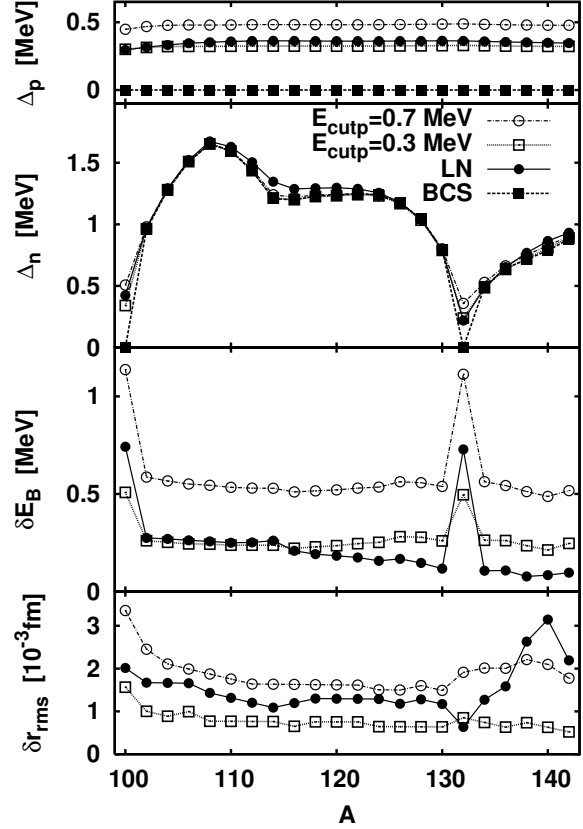


**Fig. 3.** Ground state properties for the chain of Sn isotopes computed with BCS, LN and stabilized pairing at two  $E_{\text{cutp}}$ . Upper two panels: Average proton and neutron pairing gaps. Middle panel: difference  $\delta E_B$  of binding energy from stabilized pairing or LN to the BCS binding energy. Lowest panel: difference  $\delta r_{\text{rms}}$  for the charge r.m.s.radius.

$E_{\text{cutp}}$ . Outside the magic points, the gaps from stabilized pairing come very close to the BCS values, for the small as well as for the larger cutoff, and both closer than LN.

The lower two panels in figure 3 show the effect on bulk observables. Results are drawn as difference to the BCS results in order to fit the small overall changes into a graphical representation. The changes on the total binding energy (middle panel) have an offset along all isotopes and a peak at the magic neutron numbers. Offset and peak are expected because the proton stabilization is always present and neutron stabilization adds to the effect for  $N=50$  and  $N=82$ . The average size of the modification is close to the LN values for the smaller cutoff. We have to mention, however, that the energies from LN are an uncertain quantity because the LN scheme is not variationally consistent. It is thus not fully clear what really should be plotted here. The stabilized pairing, on the other hand, has by construction a well defined energy. And a change of the order of 0.2–0.5 MeV is well acceptable in view of a typical uncertainty of 0.7–1 MeV for Skyrme forces. The effect on radii (lowest panel) is extremely small as compared to typical uncertainties of about 0.02–0.04 fm [3]. The same holds for the whole density and deduced ob-

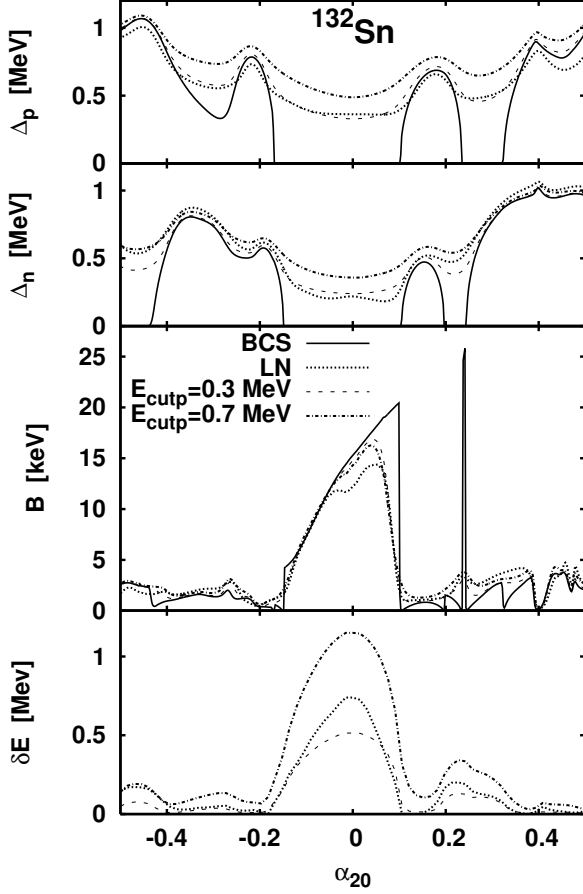


Fig. 4. Proton and neutron gaps (upper two), collective mass for motion along  $\alpha_{20}$  (middle), and difference of the collective potential from stabilized pairing or LN to that from BCS (lower) along the quadrupole deformation path for  $^{132}\text{Sn}$  computed with BCS, LN and stabilized pairing.

servables as diffraction radius and surface thickness [29, 30].

Low lying nuclear  $2^+$  states are related to large amplitude collective motion. The nucleus vibrates along a collective deformation path which consists out of a continuous series of quadrupole deformed states. The path is generated by adding a quadrupole constraint to the mean field equations sampling the various quadrupole deformations; from the given path, one can derive then the ingredients for the collective dynamics, the potential as expectation value of the energy and the collective mass from double commutators with the dynamical boost, for details see, e.g. [7, 14]. Figure 4 shows results along the axially symmetric quadrupole deformation path of  $^{132}\text{Sn}$ . BCS shows the breakdown of neutron pairing near the spherical shapes and the mass jumps immediately to large values because a pure Slater determinant is more resistant to quadrupole motion than a well pairing BCS state. The sudden changes make the BCS mass unusable for further processing in the collective Hamiltonian. LN and the stabilized functionals succeed in preventing the breakdown of pairing and in producing a smooth transition. They be-

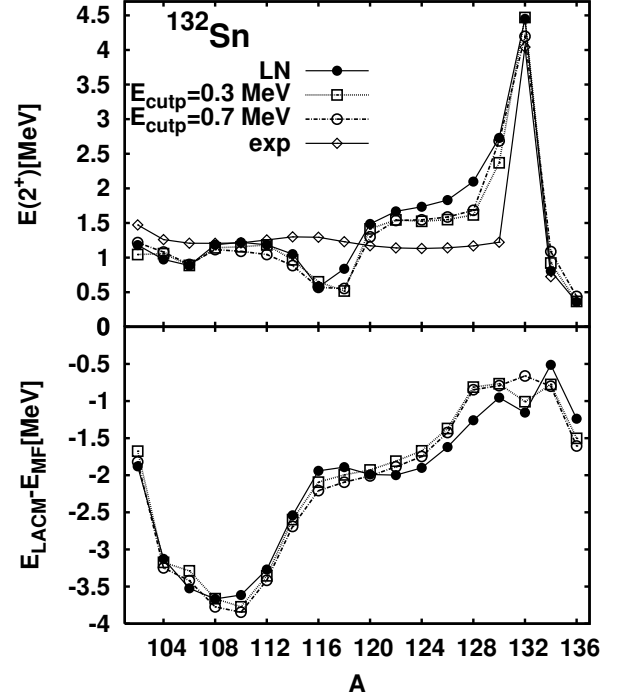


Fig. 5. Systematic of quadrupole-collective properties along the chain of Sn isotopes computed with LN and stabilized pairing at two  $E_{\text{cutp}}$ . Upper: The low-lying  $E(2_1^+)$  excitation energies. Lower: Collective correlation energies.

have similar what the collective mass and the changes in energy is concerned. It is to be noted that the stabilized pairing remains closer to the BCS mass in the regime of shell closure. The net effect of all these small differences on the collective excitations will be an average over all deformations.

Figure 4 has shown the impact of the stabilized pairing functional and its  $E_{\text{cutp}}$  on the constituents of the collective Hamiltonian, mass and potential. Figure 5 shows the net effect on the final states. The results for LN and stabilized pairing are again similar in general with a few interesting differences in detail. The sudden reduction of the  $E(2_1^+)$  when departing from the magic  $N = 82$  is very badly reproduced by LN which produces a much smoothed transition. The stabilized pairing performs better in that respect. The mid-shell level is reached already at  $N = 78$  and  $N = 80$  also does a larger down-step. The trend is the better reproduced the lower  $E_{\text{cutp}}$ . The excitation energies at the magic point and mid-shell are similar for all methods which proves that the modified pairing recipes do not affect too much the physics of the collective excitations. The sometimes larger effects seen in the details of collective mass and potential (figure 4) seem to average out in the final collective energies. The results for the correlation energies are even more robust. The values differ in tiny detail, but that is not significant because the correlation energy is anyway a small correction to the total energy.



The most important result concerns a practical aspect, not shown in the above figures: Stabilized pairing is simpler to implement numerically and it produces a faster and much more stable iteration. This amounts to a factor three faster computation of the collective deformation paths which is a substantial gain for large scale applications.

## 5 Conclusions

We have investigated a new scheme to smoothen the pairing phase transition in nuclei. The stabilized pairing is achieved by modifying the pairing functional such that the pairing energy diverges for vanishing gap. The modification is restricted to the regime of small coupling and has little effect elsewhere. The intended effect should come out similar to what is usually achieved by the Lipkin-Nogami (LN) scheme.

The operation of the stabilized functional was demonstrated in a schematic two-level model and compared to the LN. It was shown that a smooth transition to vanishing gap can indeed be achieved by the stabilized pairing functional while the convergence towards BCS results in the well pairing regime is even somewhat faster for stabilized pairing as compared to LN. The BCS ground state with stabilized pairing can also serve very well as starting point for subsequent particle number projection. The results come very close to fully fledged mean-field variation after projection.

The stabilized functional has been applied to a bunch of realistic nuclear structure calculations, ground states of spherical nuclei and low-energy collective dynamics. All results show that stabilized pairing is a valid alternative to LN. The effects are very similar in general. There are some small differences in detail which give a slight preference to stabilized pairing.

The results depend somewhat on the cutoff parameter inherent in the model. Pairing properties are, of course, more sensitive, but bulk properties, fortunately, not so much. A good choice which has small side-effects and comes in many aspects close to LN is a small value around  $E_{\text{cutp}} = 0.3\text{MeV}$ .

The major advantages of stabilized pairing lie in a formal and in a numerical feature. The formal advantage is a thoroughly variational formulation. The modification is done only at the side of the functional which provides a clean definition of the energy. The numerical gain is dramatic. Stabilized pairing provides factor three faster convergence than with LN due to the simpler algorithm possible (remaining practically identical to the robust BCS scheme). This is the strongest argument in favor of the new scheme. A stabilized pairing functional with fully variational formulation will become inevitable in future time-dependent applications where a possible phase transition would be disastrous and where LN is not applicable.

## acknowledgments

That work was supported by the BMBF contract number 06 ER 124. We thank J. Maruhn (Frankfurt) for inspiring and instructive discussions.

## References

1. Å. Bohr, B.R. Mottelson, D. Pines, Phys. Rev. **110**, 936 (1958)
2. P. Ring, P. Schuck, *The Nuclear Many-Body Problem* (Springer-Verl., New York, Heidelberg, Berlin, 1980)
3. M. Bender, P.H. Heenen, P.G. Reinhard, Rev. Mod. Phys. **75**, 121 (2003)
4. D.H.E. Gross, Phys. Rep. **279**, 119 (1997)
5. J. Dobaczewski, M.V. Stoitsov, W. Nazarewicz, P.G. Reinhard, Phys. Rev. C **76**, 054315 (2007)
6. M. Brack, J. Damgård, A.S. Jensen, H.C. Pauli, V.M. Strutinsky, C.Y. Wong, Rev. Mod. Phys. **44**, 320 (1972)
7. P.G. Reinhard, K. Goeke, Rep. Prog. Phys. **50**, 1 (1987)
8. C. Simenel, P. Chomaz, Phys. Rev. C **68**, 024302 (2003)
9. L. Guo, J.A. Maruhn, P.G. Reinhard, Phys. Rev. C **76**, 014601 (2007)
10. H.J. Lipkin, Ann. Phys. (NY) **9**, 272 (1960)
11. Y. Nogami, Phys. Rev. **B134**, 313 (1964)
12. P.H. Heenen, R.V.F. Janssens, Phys. Rev. C **57**, 159 (1998)
13. A. Valor, J.L. Egido, L.M. Robledo, Nucl. Phys. **A665**, 46 (2000)
14. P. Fleischer, P. Klüpfel, P.G. Reinhard, J.A. Maruhn, Phys. Rev. C **70**, 054321 (2004)
15. M. Bender, G.F. Bertsch, P.H. Heenen, Phys. Rev. C **73**, 034322 (2006)
16. P.G. Reinhard, W. Nazarewicz, M. Bender, J.A. Maruhn, Phys. Rev. C **53**, 2776 (1996)
17. P.G. Reinhard, M. Bender, K. Rutz, J. Maruhn, Z. Phys. A **358**, 277 (1997)
18. B.D. Serot, J.D. Walecka, Adv. Nucl. Phys. **16**, 1 (1986)
19. P.G. Reinhard, Rep. Prog. Phys. **52**, 439 (1989)
20. P. Ring, Prog. Part. Nucl. Phys. **37**, 193 (1996)
21. J. Dechargé, D. Gogny, Phys. Rev. **C21**, 1568 (1980)
22. J. Dobaczewski, H. Flocard, J. Treiner, Nucl. Phys. **A422**, 103 (1984)
23. F. Tondeur, Nucl. Phys. **A315**, 353 (1979)
24. S.J. Krieger, P. Bonche, H. Flocard, P. Quentin, M.S. Weiss, Nucl. Phys. **A517**, 275 (1990)
25. M. Bender, K. Rutz, P.G. Reinhard, J.A. Maruhn, Eur. Phys. J. **A8**, 59 (2000)
26. J. Stone, P.G. Reinhard, Prog. Part. Nucl. Phys. **58**, 587 (2007)
27. P.G. Reinhard, in *Computational Nuclear Physics 1 – Nuclear Structure*, edited by K. Langanke, J.A. Maruhn, S.E. Koonin (Springer, Berlin, Heidelberg, New York, 1991), pp. 28–50
28. P.G. Reinhard, H. Flocard, Nucl. Phys. **A584**, 467 (1995)
29. J. Friedrich, N. Vögler, Nucl. Phys. **A373**, 192 (1982)
30. J. Friedrich, P.G. Reinhard, Phys. Rev. C **33**, 335 (1986)